Anal. Chem. **2004,** *76,* 2281−2289

Scanning Electrochemical Microscopy 50. Kinetic Study of Electrode Reactions by the Tip Generation−Substrate Collection Mode

José L. Fernández and Allen J. Bard*

Department of Chemistry and Biochemistry, The University of Texas at Austin, Austin, Texas 78712

A scanning electrochemical microscopy (SECM) methodology for localized quantitative kinetic studies of electrode reactions based on the tip generation−substrate collection (TG−SC) operation mode is presented. This approach does not use the mediator feedback required in typical kinetic SECM experiments. The reactant is galvanostatically electrogenerated on a tip placed in proximity to the substrate. It diffuses through the tip−substrate gap and undergoes the reaction of interest on the substrate surface. The substrate current is monitored with time until it reaches an apparent steady-state value. The process was digitally simulated using an explicit finite difference method, for an irreversible first-order electrode reaction at the substrate. Transient responses, steady-state polarization curves, and TG−SC approach curves can be used to obtain substrate kinetics. The effects of the experimental parameters were analyzed. The possibility of easily changing the experimental conditions with the SECM is an attractive approach to obtain independent evidence that can be used for a strict test of reaction mechanisms. The technique was applied for a preliminary simplified kinetic examination of the oxygen reduction reaction in phosphoric acid.

Scanning electrochemical microscopy (SECM) is a powerful technique for studying kinetics of heterogeneous electron-transfer reactions.[1] Several reactions have been analyzed mainly using the amperometric feedback mode.[2−10] In this operation mode, kinetic information is extracted from the tip current as the mediator couple in solution reacts at tip and substrate. The mediator generates the reactant of the reaction of interest on the substrate through a diffusion-controlled reaction at an ultramicroelectrode (UME) tip. The electrogenerated reactant diffuses in the tip−substrate gap and regenerates the mediator at the substrate surface. The change in the mediator concentration caused by this process is detected by the UME tip because of the proportionality between the diffusion tip current and the mediator concentration.[11] One condition for this approach to be used is that the initial mediator concentration must be sufficiently small that the tip reaction operates under diffusion control. Thus, the conditions where it is possible to perform kinetic measurements by SECM are limited in the range of mediator concentrations where positive feedback can be detected.

Other SECM operation modes, like those based on generation−collection configurations, have been used less often for studying electrode reactions.[12−14] The substrate generation−tip collection (SG−TC) mode is very convenient for obtaining information about localized electrode processes on heterogeneous surfaces.[12,13] On the other hand, the tip generation−substrate collection (TG−SC) mode has been useful in studying coupled homogeneous chemical reactions in electrode reactions.[15−17]

Recently, we suggested a modification of the TG−SC mode and demonstrated its application for imaging electrocatalytic activity.[18] This configuration does not require tip feedback and is thus appropriate for studying electrode reactions under conditions that are inaccessible to the conventional feedback mode, such as oxygen reduction and hydrogen oxidation in acidic and alkaline media, respectively. The ability of this mode for imaging activity has already been verified,[18] although a detailed theoretical analysis of the process is needed to make use of this configuration for obtaining quantitative kinetic information. Although most of the SECM configurations have been theoretically treated,[2,15,17,19−27]

* Corresponding author. E-mail: ajbard@mail.utexas.edu.

(1) *Scanning Electrochemical Microscopy*; Bard, A. J., Mirkin, M. V., Eds.; Marcel Dekker: New York, 2001.
(2) Bard, A. J.; Mirkin, M. V.; Unwin, P. R.; Wipf, D. O. *J. Phys. Chem.* **1992**, *96*, 1861.
(3) Mirkin, M. V.; Richards, T. C.; Bard, A. J. *J. Phys. Chem.* **1993**, *97*, 7672.
(4) Horrocks, B. R.; Mirkin, M. V.; Bard, A. J. *J. Phys. Chem.* **1994**, *98*, 8, 9106.
(5) Tsionsky, M.; Bard, A. J.; Mirkin, M. V. *J. Phys. Chem.* **1996**, *100*, 17881.
(6) Zhou, J.; Zu, Y.; Bard, A. J. *J. Electroanal. Chem.* **2000**, *491*, 22.
(7) Jambunathan, K.; Shah, B. C.; Hudson, J. L.; Hillier, A. C. *J. Electroanal. Chem.* **2001**, *500*, 279.
(8) Ding, Z.; Quinn, B. M.; Bard, A. J. *J. Phys. Chem. B* **2001**, *105*, 6367.
(9) Miao, W.; Ding, Z.; Bard, A. J. *J. Phys. Chem. B* **2002**, *106*, 1392.
(10) Liu, B.; Bard, A. J. *J. Phys. Chem. B* **2002**, *106*, 12801.
(11) Wightman, R. M.; Wipf, D. O. In *Electroanalytical Chemistry*; Bard, A. J., Ed.; Marcel Dekker: New York, 1989; Vol. 15, pp 267−353.
(12) Engstrom, R. C.; Small, B.; Kattan, L. *Anal. Chem.* **1992**, *64*, 241.
(13) Basame, S. B.; White, H. S. *J. Phys. Chem. B* **1998**, *102*, 9812.
(14) Lee, C.; Kwak, J.; Anson, F. C. *Anal. Chem.* **1991**, *63*, 1501.
(15) Zhou, F.; Unwin, P. R.; Bard, A. J. *J. Phys. Chem.* **1992**, *96*, 4917.
(16) Treichel, D. A.; Mirkin, M. V.; Bard, A. J. *J. Phys. Chem.* **1994**, *98*, 5751.
(17) Demaille, C.; Unwin, P. R.; Bard, A. J. *J. Phys. Chem.* **1996**, *100*, 14137.
(18) Fernández, J. L.; Bard, A. J. *Anal. Chem.* **2003**, *75*, 2967.
(19) Kwak, J.; Bard, A. J. *Anal. Chem.* **1989**, *61*, 1221.
(20) Bard, A. J.; Denuault, G.; Friesner, R. A.; Dornblaser, B. C.; Tuckerman, L. S. *Anal. Chem.* **1991**, *63*, 1282.
(21) Martin, R. D.; Unwin, P. R. *J. Chem. Soc., Faraday Trans.* **1998**, *94*, 753.
(22) Amphlett, J. L.; Denuault, G. *J. Phys. Chem. B* **1998**, *102*, 9946.
(23) Galceran, J.; Cecília, J.; Companys, E.; Salvador, J.; Puy, J. *J. Phys. Chem. B* **2000**, *104*, 7993.
(24) Selzer, Y.; Mandler, D. *Anal. Chem.* **2000**, *72*, 2383.
(25) Fulian, Q.; Fisher, A. C.; Denuault, G. *J. Phys. Chem. B* **1999**, *103*, 4387.
(26) Lee, Y.; Amemiya, S.; Bard, A. J. *Anal. Chem.* **2001**, *73*, 2261.

10.1021/ac035518a CCC: $27.50
Published on Web 03/20/2004

simulations dealing with the tip operating at constant current have never appeared. We present here a theoretical analysis of this system operating with an irreversible first-order reaction at the substrate. This is the simplest model for addressing the kinetics of an electrode process. The analysis includes transient and steady-state simulations performed using an explicit finite difference method (FDM).[28] The effects of geometric and experimental parameters on the expected responses as well as the capabilities and limitations of this configuration were evaluated. The method was further applied to a kinetic study of the oxygen reduction reaction (ORR) on platinum in an acidic medium.

EXPERIMENTAL DETAILS

Preparation of Electrodes. Pt 25-μm-diameter UME tips were prepared by the conventional heat-sealing and mechanical-sharpening procedures previously described.[1] Pt disks (with 127-, 50-, 25-, and 10-μm diameters) that were used as substrates were prepared by heat-sealing Pt wires (Aldrich, Milwaukee, WI) in borosilicate glass capillaries by the same procedure that was used for the tips. These electrodes were encased in Teflon cylindrical sheaths polished with alumina powder (down to 0.05 μm) and ultrasonically cleaned. They were cleaned by immersion in acidic hydrogen peroxide (10% v/v) for 1 h before the experiments.

Electrochemical Measurements. Measurements were made in deaereated 0.5 M H_3PO_4 (pH = 1.5) (Fisher, Fair Lawn, NJ) at room temperature using the SECM setup previously described.[18] A hydrogen reference electrode was prepared with a platinized Pt wire in 0.5 M H_3PO_4 saturated with H_2 (1 atm). The potential of this electrode against the normal hydrogen electrode (NHE) is −0.09 V. A Pt wire was the auxiliary electrode. A CHI 900 SECM instrument (CH Instruments, Austin, TX) was used. The tip current was controlled with a floating power source (9 V) connected between the tip (positive) and the auxiliary electrode. Tip currents were measured by reading the potential drop across a calibrated resistor connected in series to the power source circuit. All the potential values in this work will be referred to the NHE.

The tip was placed close to the substrate by using the negative feedback for the reduction of oxygen (tip potential $E_T = 0.2$ V) in nondeaereated 0.5 M H_3PO_4. Total negative feedback theoretical curves correctly fit these approach curves allowing the precise positioning of the tip close to the substrate. Fitting of these curves also permitted an estimation of RG (= r_g/a, where a and r_g are the Pt disk and overall tip radius including the insulating glass sheath, respectively) of the tips used in this work.[1] To place the tip exactly over the Pt disk, TG−SC images for the ORR were obtained by the procedure previously described.[18] They were performed at a tip−substrate distance $d = 30$ μm, using a tip current $i_T = -80$ nA and holding the substrate potential (E_S) at 0.2 V.

Steady-state substrate current (i_S^{SS}) versus E_S curves were measured between 0.1 and 0.95 V versus NHE. Before taking each point, the substrate was electrochemically cycled between 1.35 and −0.09 V at 0.5 V/s[29] until reproducible voltammograms were obtained. Each (i_S^{SS}, E_S) point was measured by the chrono-amperometric method previously used.[18] Tip currents that were used in this work spanned in the range 20 nA ≤ $|i_T|$ ≤ 350 nA.

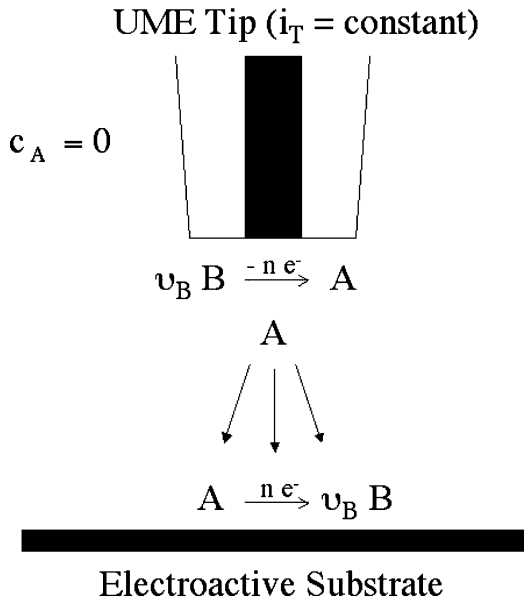

Figure 1. Scheme of the modified TG−SC mode of SECM used for kinetic studies of electrode reactions.

THEORETICAL BASIS

Description of the System. The scheme in Figure 1 shows the basic principles of the method. The substrate is held at a potential where the reaction studied (eq 1) should occur in the

$$\mathrm{A} + n\mathrm{e}^- \underset{\text{tip}}{\overset{\text{substrate}}{\rightleftharpoons}} \upsilon_B\mathrm{B} \qquad (1)$$

forward direction. However, since the concentration of reactant (or species A) is initially very small, the substrate current is negligible. An UME tip in proximity to the substrate electrogenerates A from B through the reverse of reaction 1 at constant current, so a constant flux of A is produced. The concentration of B is high enough to remain unchanged during the process.

During the experiment, a concentration profile of A develops from the tip toward the substrate because of the diffusion of A. When A reaches the electroactive substrate surface, it undergoes the electrode reaction of interest (eq 1). Under activated or mixed (kinetic diffusion) conditions, the substrate current (i_S) depends on the kinetic parameters of the reaction, on E_S, and on the concentration profile of A at the substrate surface. The latter also depends on the geometric parameters, such as d, RG of the tip, and the substrate-to-tip radius ratio (STR = a_S/a). The interdependence of these variables is complex, and an analytical solution of this system would be difficult to obtain. In this context, simulations can provide a more straightforward tool to relate i_S with the kinetic parameters of the reaction addressing the effects of all the geometric variables.

Model for FDM Simulations. The TG−SC process was treated by two-dimensional FDM simulations[28] in cylindrical coordinates. This numerical method is slower than others that have been used to treat SECM problems,[1] but the availability and

(27) Liljeroth, P.; Johans, C.; Slevin, C. J.; Quinn, B. M.; Kontturi, K. *Anal. Chem.* **2002**, *74*, 1972.
(28) Feldberg, S. W. In *Electroanalytical Chemistry*; Bard, A. J., Ed.; Marcel Dekker: New York, 1969; Vol. 3, pp 199−296.
(29) Johnson, D. C.; Bruckenstein, S. *Anal. Chem.* **1971**, *43*, 1313.

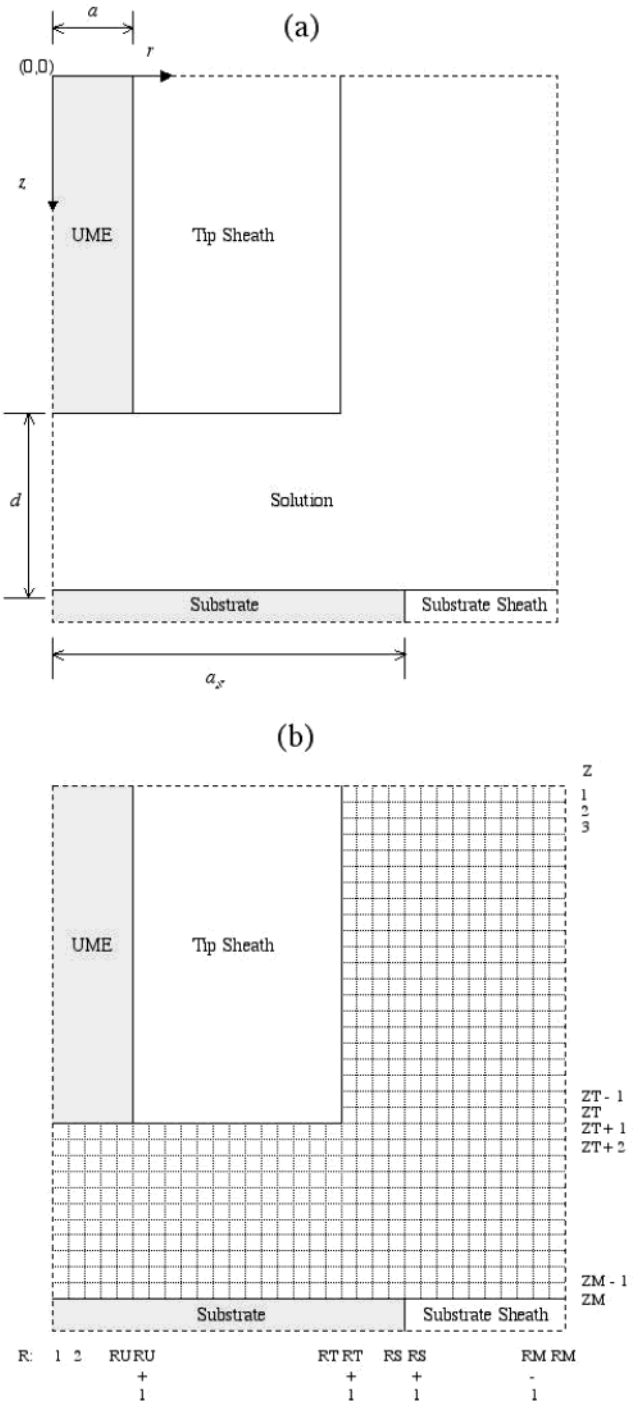

Figure 2. (a) Model of the SECM system to simulate the TG−SC operation mode. (b) Discrete model for the FD simulation of the TG−SC operation mode.

speed of current computers make this problem less important. Furthermore, its simplicity and flexibility make it an intuitive and versatile calculation technique for a number of other SECM problems.

A scheme of the model is shown in Figure 2a. Symmetry around the axis $r = 0$ is assumed (axis−symmetric system). The tip is a cylinder, and the substrate is completely smooth and parallel to the UME surface. The model considers a finite-radius tip sheath, so one must consider "back region" diffusion toward the bulk solution. The substrate has a finite radius and is also surrounded by an insulating sheath.

The system presented in Figure 2a is mapped into ring-shaped boxes of thickness Δr and height Δz, as shown in Figure 2b. The box-face areas ($A^{Z,R}$), given by eqs 2−4, are important for evaluating the flux across the boundary between two boxes.

$$A^{Z,R-} = 2\pi(R - 1)\Delta r\Delta z \quad (2)$$

$$A^{Z,R+} = 2\pi R\Delta r\Delta z \quad (3)$$

$$A^{Z-,R} = A^{Z+,R} = \pi(2R - 1)\Delta r^2 \quad (4)$$

where the superscripts $R+/R-$ and $Z+/Z-$ refer to inner/outer and up/down areas, respectively, for the ring box Z, R. Furthermore, the box volume ($V^{Z,R}$) is given by eq 5.

$$V^{Z,R} = \pi(2R - 1)\Delta r^2\Delta z \quad (5)$$

The net flux of A through a box Z, R ($J_A^{Z,R}$) results from the sum of all processes involving mass change into this box. In this case, it can be calculated according to eq 6,

$$J_A^{Z,R} = j_A^{Z,R-}A^{Z,R-} - j_A^{Z,R+}A^{Z,R+} + j_A^{Z-,R}A^{Z-,R} - j_A^{Z+,R}A^{Z+,R} \quad (6)$$

where $j_A^{Z,R}$ is the flux density at each box border, which depends on the boundary conditions at the particular location. On the other hand, the finite temporal change of concentration into a box ($c_A^{Z,R}$), according to the definition of flux, is given by eq 7

$$c_A^{*Z,R} - c_A^{Z,R} = (J_A^{Z,R}\Delta t)/V^{Z,R} \quad (7)$$

where the superscript * indicates the new concentration value after the period of time Δt.

The combination of eqs 2−7, together with the boundary conditions, allows the evaluation of the concentration in each box after a finite period of time. Table 1 presents the initial and boundary conditions governing the fluxes of A across each box boundary for the TG−SC model treated. The first two conditions consider the initial absence of A in the solution and the invariability of the concentration of B, respectively. The third condition establishes the outer boundaries of the simulated system by applying the infinite-distance condition. The flux of A across the tip|solution boundary is constant, being zero on the tip glass sheath and related to the tip current density (j_T) on the UME. In this last case, the effect of current distribution on the UME is neglected, since actually j_T is a function of the radius. This approximation is acceptable provided that j_T is low. The flux of A across the solution|substrate boundary is null on the substrate sheath and governed by the kinetics of reaction 1 on the conductive disk. In this work, the simplest situation of an irreversible substrate reaction is treated. Thus, the Butler−Volmer equation without the reverse term, first order in the concentration of A, is used for modeling the substrate electrode reaction. The kinetic constant k depends on the standard reaction rate constant (k_o) and E_S through eq 8,[30] where $E°$ is the standard potential of reaction 1, α is the transfer coefficient, and $f = 38.92\ V^{-1}$ at 25

(30) *Electrochemical Methods: Fundamental and Applications*; Faulkner, L. R., Bard, A. J., Eds.; Wiley: New York, 2001.

Table 1. Initial and Boundary Conditions in the FD System for the TG−SC SECM Model

time	grid limits	condition
$t = 0$	$1 \le R$, ZT $\le Z \le$ ZM RG $+ 1 \le R$, $Z \le$ ZT $- 1$	$c_A^{Z,R} = 0$
$t \ge 0$	$1 \le R$, ZT $\le Z \le$ ZM RG $+ 1 \le R$, $Z \le$ ZT $- 1$	$c_B^{Z,R} = c_B^{o}$
$t > 0$	RM $< R$, $1 \le Z \le$ ZM RG $+ 1 \le R \le$ RM, $Z < 1$	$c_A^{Z,R} = 0$
	$1 \le R \le$ RT, $Z =$ ZT $+ 1$	$j_A^{Z-,R} = \begin{cases} -\dfrac{j_T}{nF}, & R \le RU \\ 0, & RU + 1 \le R \le RT \end{cases}$
	$1 \le R \le$ RM, $Z =$ ZM	$j_A^{Z+,R} = \begin{cases} -kc_A^{ZM,R}, & R \le RS \\ 0, & RS + 1 \le R \le RM \end{cases}$
	$R = 1$, ZT $+ 1 \le Z \le$ ZM $R =$ RG $+ 1$, $1 \le Z \le$ ZT	$j_A^{Z,R-} = 0$
		$j_A^{Z-,R} = -\dfrac{D_A(c_A^{Z,R} - c_A^{Z-1,R})}{\Delta z}$
		$j_A^{Z+,R} = -\dfrac{D_A(c_A^{Z+1,R} - c_A^{Z,R})}{\Delta z}$
	through any other box boundary	$j_A^{Z,R-} = -\dfrac{D_A(c_A^{Z,R} - c_A^{Z,R-1})}{\Delta r}$
		$j_A^{Z,R+} = -\dfrac{D_A(c_A^{Z,R+1} - c_A^{Z,R})}{\Delta r}$

$$k = k_o e^{-\alpha f(E_S - E^\circ)} \tag{8}$$

°C.[30] Finally, Fick's first law governs the diffusion of A across the rest of box boundaries, where D_A is the diffusion coefficient of A.

By applying the conditions in Table 1 to eqs 6 and 7, the concentrations of A in each box after a finite time interval Δt can be calculated. Starting from the initial conditions and doing successive iterations it is possible to obtain the simulated time-dependent concentration profile. Furthermore, the time dependence of the substrate current can be calculated from eq 9, using the concentrations of A in the boxes over the substrate surface.

$$i_S = nF \sum_{R=1}^{R=RS} j_A^{ZM+,R} A^{ZM+,R} = nF\pi\Delta r^2 \sum_{R=1}^{R=RS} (2R - 1) j_A^{ZM+,R} \tag{9}$$

Dimensionless Parametrization. Simulations using dimensionless parameters are more general. Most of the parameters in this model may be normalized in the same way as in other UME simulations.[2,31] However, normalization of the concentration is not direct in this case because the bulk concentration of A, which is conventionally used for this purpose, is zero. Nevertheless, it is possible to relate the tip current value with an apparent concentration of A ($c_A^{\#}$) according to eq 10. Just to relate this value with a

$$i_T = -nF\pi D_A a c_A^{\#} \tag{10}$$

physical meaning, it could be associated with the time-dependent actual concentration of A at the UME surface and thickness of the diffusion layer.

Table 2 shows the normalized fluxes and parameters used to perform the calculation with eqs 2−7. The normalization of eq 9 leads to eq 11. Note that, for a first-order irreversible reaction,

$$Ni_S = \Delta Nr^2 \sum_{R=1}^{R=RS} (2R - 1) N j_A^{ZM+,R} \tag{11}$$

the normalized TG−SC responses should not depend on the magnitude of the tip current.

The algorithm was programmed using Fortran 77 language. Simulations were carried out using grids with $\Delta Nr = \Delta Nz = 0.04$ (RU = 25) and $\Delta Nt = 3 \times 10^{-4}$. Iterations were done until the variation of Ni_S was smaller than 10^{-8} step^{-1}, which was considered a quasi-steady-state situation. RG was varied between 2 and 10, and the number of UME radii in the back region was kept to 10. The number of boxes in the z direction changed depending on the value of L, but usually ZT = 100 and ZM ≤ 300. Each complete calculation lasted no more than 1 h with a PC (2.4 GHz, 512 MB RAM), which is acceptable taking into account that no attempt was made to optimize the calculation time (e.g., by using an expanding grid[22,31]).

RESULTS AND DISCUSSION

Check of the Algorithm. Simulations were checked in three different ways. First, the correctness of the algorithm formulation was corroborated using the limiting case where the substrate reaction is rapid enough to operate under total mass-transfer control, the substrate is infinite, the tip RG is large, and the tip is very close to the substrate ($L < 1$). For these conditions, the

(31) Fang, Y.; Leddy, J. *Anal. Chem.* **1995**, *67*, 1259.

Table 2. Initial and Boundary Conditions in the FD System for the Dimensionless TG−SC SECM Model

normalized parameters

$$\Delta Nr = \frac{\Delta r}{a};\ \Delta Nz = \frac{\Delta z}{a};\ Nt = \frac{D_A t}{a^2};\ L = \frac{d}{a}$$

$$Nc_A^{Z,R} = \frac{c_A^{Z,R}}{c_A^{\#}};\ Nk = \frac{ka}{D_A};\ Ni_S = \frac{i_S}{i_T};\ Nj_A^{Z,R} = \frac{j_A^{Z,R}}{j_A^{(ZT+1)-,(R\le RU)}}$$

grid limits	condition
$1 \le R \le \mathrm{RT},\ Z = \mathrm{ZT} + 1$	$Nj_A^{Z-,R} = \begin{cases} -1 & R \le RU \\ 0 & RU + 1 \le R \le RT \end{cases}$
$1 \le R \le \mathrm{RM},\ Z = \mathrm{ZM}$	$Nj_A^{Z+,R} = \begin{cases} NkNc_A^{ZM,R} & R \le RS \\ 0 & RS + 1 \le R \le RM \end{cases}$
$R = 1,\ \mathrm{ZT} + 1 \le Z \le \mathrm{ZM}$ $R = \mathrm{RG} + 1,\ 1 \le Z \le \mathrm{ZT}$	$Nj_A^{Z,R-} = 0$
through any other box boundary	$Nj_A^{Z-,R} = -\frac{(Nc_A^{Z,R} - Nc_A^{Z-1,R})}{\Delta Nz}$
	$Nj_A^{Z+,R} = -\frac{(Nc_A^{Z+1,R} - Nc_A^{Z,R})}{\Delta Nz}$
	$Nj_A^{Z,R-} = -\frac{(Nc_A^{Z,R} - Nc_A^{Z,R-1})}{\Delta Nr}$
	$Nj_A^{Z,R+} = -\frac{(Nc_A^{Z,R+1} - Nc_A^{Z,R})}{\Delta Nr}$

expected[15] $Ni_S^{SS} = 1$ was obtained. This condition is very sensitive to slight errors in the algorithm. Second, it was verified that the temporal and spatial resolution is sufficient by checking the consistency of the results as the number of boxes in the grid was increased. This happens for RU ≥ 13, which means $\Delta Nr \le 0.08$. The same situation was found for ΔNz. Third, the accuracy of the FD method was evaluated by performing simulations of approach curves under kinetic feedback conditions. The results were compared with those already obtained by other methods.[2] It was necessary to change the boundary conditions at the tip and to include the tip−substrate diffusion loop of species B. A difference of less than 0.2% was achieved when using RU = 25 over the same range of L as was used for the TG−SC simulations ($L \le 8$).

Transient and Steady-State Simulations. Figure 3 shows transients of the normalized substrate current (or collection efficiency) for different reaction rates at the substrate in a typical simulated TG−SC experiment. There is a delay time where $Ni_S = 0$, which is the time for A to arrive at the substrate surface after traveling across the tip−substrate gap. This is typical of generation−collection experiments.[15] After that time, Ni_S increases with a reaction rate-dependent slope. The rise time to reach a steady-state value is strongly sensitive to the reaction rate, being of the order of milliseconds when the reaction is fast and of the order of seconds when it is slow. There is a group of Nk values that yields the same Ni_S^{SS} value of 1 when the tip is near the substrate. In those cases, the reaction is so fast that it is operating under total diffusion control, maintaining the concentration of A at the substrate surface close to zero. The steady-state concentration profile for this situation is shown in Figure 4a. The dispersion of A does not go beyond twice the UME radius and is essentially

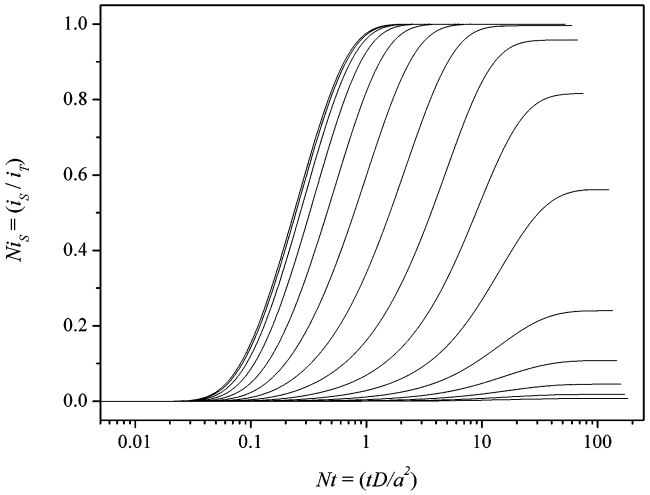

Figure 3. Dependence of the normalized substrate current on the normalized time in simulated TG−SC experiments with different rate constants at the substrate. Conditions: L = 0.8, RG = 10, STR = 10. From top to bottom curves, Nk = 100, 40, 16, 6.4, 2.56, 1.024, 0.4096, 0.1638, 6.554 × 10^{-2}, 2.621 × 10^{-2}, 1.05 × 10^{-2}, 4.19 × 10^{-3}, 1.68 × 10^{-3}, 6.71 × 10^{-4}, and 2.68 × 10^{-4}.

independent of RG for RG > 2, in accordance with previous TG−SC simulations.[15] Even at steady state, the reaction operates under diffusion control ($Ni_S^{SS} \cong 1$), the time response depends on the kinetic parameters. Thus, the transient responses could be used for studying fast reactions. Below a given reaction rate value, the kinetics of the substrate reaction begins to affect the steady-state behavior. In this case, Ni_S^{SS} is lower than 1 and decreases when Nk decreases. On the other hand, as can be seen in Figure 4b and c for two extreme RG values, geometric parameters have more

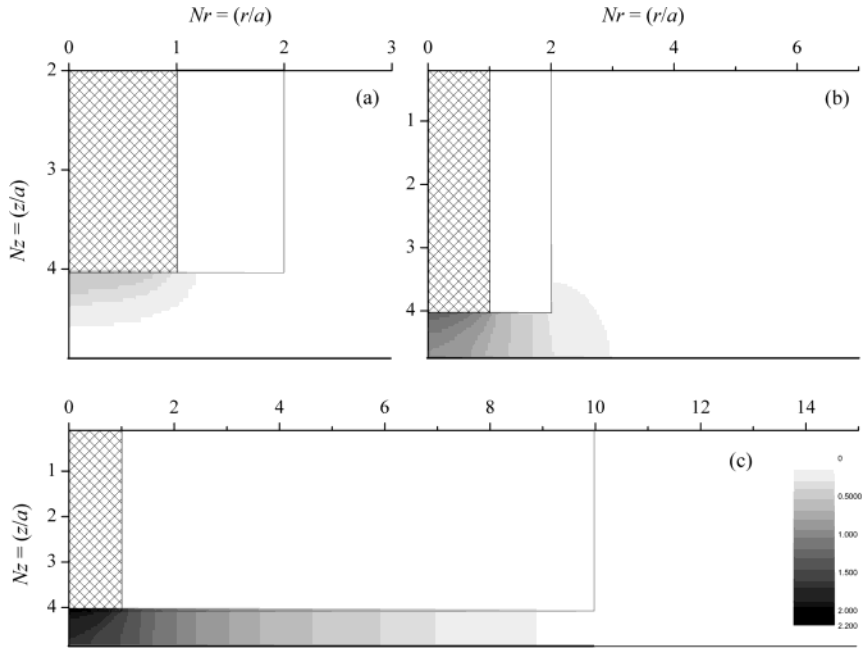

Figure 4. Simulated quasi-steady-state normalized concentration profiles of A in TG−SC experiments. Conditions: $L = 0.8$, STR = 10; (a) RG = 2, $Nk = 100$; (b) RG = 2, $Nk = 2.68 \times 10^{-4}$; (c) RG = 10, $Nk = 2.68 \times 10^{-4}$. The gray scale, common to the three graphs, relates the values of normalized concentrations with the gray map.

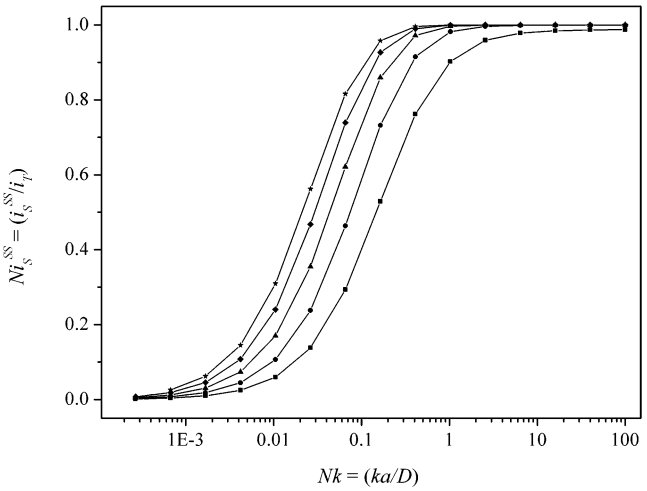

Figure 5. Dependence of the normalized steady-state substrate current on the normalized rate constant in simulated TG−SC experiments with different RG values. Conditions: $L = 0.8$, STR = 10; RG = 2 (■), 4 (●), 6 (▲), 8 (◆), and 10 (★).

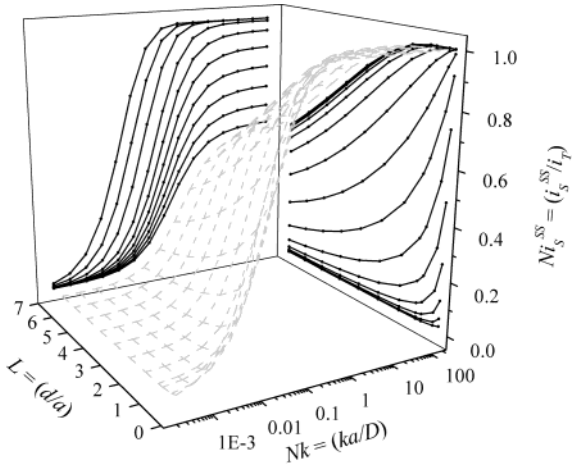

Figure 6. Dependence of the normalized steady-state substrate current on the normalized rate constant and on the normalized tip−substrate distance in simulated TG−SC experiments. Conditions: STR = 5, RG = 10. Projections on the Ni_S^{SS}−Nk plane from top to bottom, L = 0.2, 0.4, 0.8, 1.6, 2.4, 3.2, 4.0, 4.8, 5.6, and 6.4. Projections on the Ni_S^{SS}−L plane from top to bottom, Nk = 100, 40, 16, 6.4, 2.56, 1.024, 0.4096, 0.1638, 6.554×10^{-2}, 2.621×10^{-2}, 1.05×10^{-2}, 4.19×10^{-3}, 1.68×10^{-3}, 6.71×10^{-4}, and 2.68×10^{-4}.

significant effects on the concentration profiles and, consequently, on the Ni_S^{SS} values. Thus, a more detailed analysis of the effect of these parameters is necessary to obtain a good interpretation of the experimental results.

Figures 5 and 6 show the dependences of Ni_S^{SS} on Nk for different geometric conditions. Note that the Ni_S^{SS} versus Nk curves contain the same information as classical polarization curves (i vs E), since $Nk = Nk(E)$. Thus, another way to perform kinetic studies with this technique is to correlate the experimental polarization curves with the simulated ones. The effect of RG on the polarization curves, as shown in Figure 5, is mainly significant in the region where the kinetic information resides. This fact will affect the accuracy of the correlated parameters, since RG is not a controlled variable. However, the RG effect is minimized when tips with large RG values (RG = 8−10) are used, where the polarization curves are very similar. Figure 6 shows that the tip−substrate distance has an effect on the polarization curves (Ni_S^{SS}−Nk plane), both in the mixed and mass-transfer regions. Furthermore, the Ni_S^{SS} versus L curves (Ni_S^{SS}−L plane) could be used both for precise positioning of the tip near the substrate and as another way to perform kinetic studies. The equivalent experiment to the total positive feedback approach curve is the situation where the substrate current is completely governed by diffusion. A family of kinetic TG−SC approach curves results when they are obtained in the mixed region from which the reaction rate constants could be calculated.

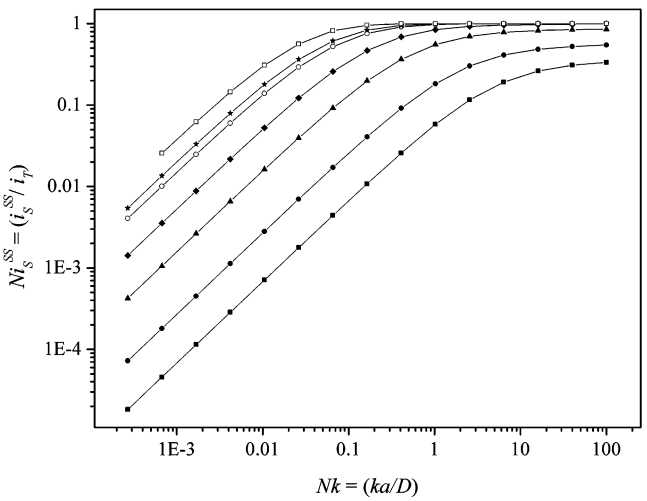

Figure 7. Dependence of the normalized steady-state substrate current on the normalized rate constant in simulated TG−SC experiments with different STR values (where STR = a_S/a, the ratio of substrate radius to tip radius). Conditions: $L = 0.8$, RG = 10; STR = 10 (□), 5 (★), 4 (○), 2 (◆), 1 (▲), 0.4 (●), and 0.2 (■).

Figure 7 shows the effect of STR, the relative size of the substrate and tip, on the polarization curves. These curves are plotted on a logarithmic scale to better reveal the strong effect of this parameter on the extension of the kinetic control region. Thus, by using a substrate with STR = 10, it would not be possible to study reactions with $Nk > 0.1$, and when STR = 0.2, the range of Nk can be extended up to values higher than 100. Furthermore, extending the kinetic range could be useful even with slow reactions, to detect processes that occur at higher overpotentials, normally masked by the mass-transfer limited response. Data plotted in Figures 5−7 are tabulated in the Supporting Information.

Study of the ORR on Pt. The reduction of oxygen to water in acidic media (eq 12) on platinum was studied as a first

$$O_2 + 4H^+ + 4e^- \rightarrow 2H_2O \qquad (12)$$

application of the proposed method. This reaction cannot be studied by the feedback mode in these conditions because the mediator is water, which has an extremely high concentration.

The ORR on Pt electrodes has been extensively studied because of its importance in many electrochemical devices, such as fuel cells, but its complex mechanism still remains uncertain. However, there is a significant amount of evidence supporting the fact that at higher overpotentials the reaction is first order with respect to the concentration of O_2.[32−35] Thus, the described model could be used to study this electrode reaction under the circumstances where this condition applies.

The reverse of (12), oxygen generation, was accomplished at the tip by polarizing it at a constant anodic current. Both the concentrations of H^+ and H_2O remained unchanged during the

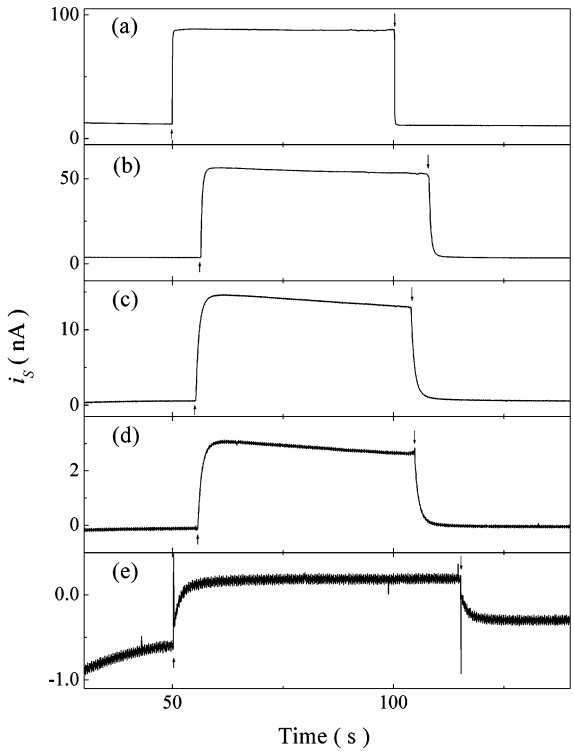

Figure 8. Typical substrate current transients obtained during an ORR TG−SC experiment on a 127-μm Pt disk using a 25-μm Pt tip. $i_T = -75$ nA, $L = 0.8$ at $E_S = 0.3$ (a), 0.74 (b), 0.81 (c), 0.85 (d), and 0.90 V (e). Up and down arrows signal the moment when the tip is turned on and off, respectively.

experiments due to their very high initial values. To calculate k from the Nk values obtained from the simulated curves, the diffusion coefficient of O_2 in phosphoric acid was taken as 1.5×10^{-5} cm^2/s.[36] The standard potential for this reaction is $E° = 1.229$ V versus NHE.[35]

Figure 8 shows the Ni_S time dependencies obtained on a Pt disk during TG−SC experiments with the ORR. Both the rising (tip on) and the decaying (tip off) responses reached apparent steady-state values for oxygen reduction and background, respectively. The steady-state currents were stable for several minutes at the higher overpotentials, but they underwent slight reproducible decays at lower overpotentials, which are caused by deactivation of the Pt electrode due to surface rearrangement.[33] Although the analysis of these transients would be advantageous in some aspects,[20] to correlate them with the simulated curves involves several problems, both instrumental and intrinsic to the experiment.[20,37] The treatment of steady-state data is more straightforward.

Steady-state polarization curves (i_S^{SS} vs E_S) were obtained. The substrate current (after background subtraction) measured 5 s after turning the tip on was plotted as a function of the substrate potential. These curves correspond to very active platinum that was electrochemically activated immediately before measuring each point. Figure 9 shows a set of polarization curves obtained using different tip currents. While the nonnormalized i_S^{SS} versus E_S curves obviously depend on i_T (Figure 9a), after normalization,

(32) Adzic, R. In *Electrocatalysis*; Lipkowski, J., Ross, P. N., Eds.; Wiley-VCH: New York, 1998; pp 197−242.
(33) Kinoshita, K. *Electrochemical Oxygen Technology*; Wiley: New York, 1992.
(34) Damjanovic, A. In *Electrochemistry in Transition*; Murphy, O. J., Srinivasan, S., Conway, B. E., Eds.; Plenum: New York, 1992; pp 107−126.
(35) Hoare, J. P. In *Encyclopedia of Electrochemistry of the Elements*; Bard, A. J., Ed.; Marcel Dekker: New York, 1974; Vol. II, pp 191−373.
(36) Lawson, D. R.; Whiteley, L. D.; Martin, C. R.; Szentirmay, M. N.; Song, J. I. *J. Electrochem. Soc.* **1988**, *135*, 2247.
(37) Bard, A. J.; Fan, F.-R. F.; Kwak, J.; Lev, O. *Anal. Chem.* **1989**, *61*, 132.

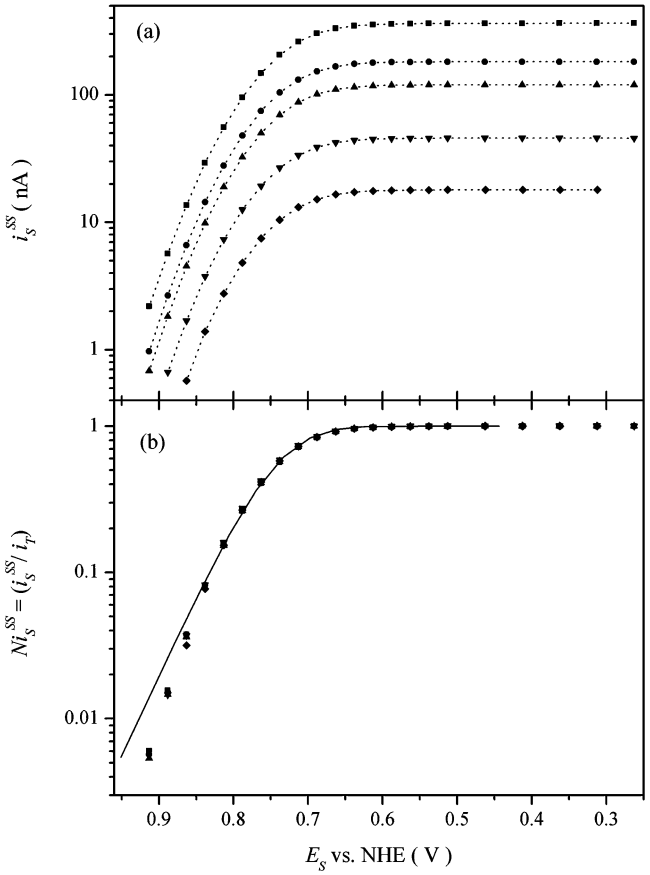

Figure 9. Dependence of the steady-state substrate current (a) and the normalized steady-state substrate current (b) on the substrate potential, obtained from ORR TG−SC experiments on a 127-μm Pt disk using a 25-μm Pt tip. $L = 0.79$, RG ≅ 10, $i_T = -19$ (◆), −35 (▼), −120 (▲), −180 (●), and −350 nA (■). Solid line: simulation (see Table 3). Experimental substrate currents calculated as the net current read at ∼5 s into the step minus the value of the background projection at the same time.

they all converge into a single curve (Figure 9b). This confirms that the ORR is operating by a first-order reaction with respect to the concentration of O_2 in the analyzed range of potentials ($0.65 < E$ (V) < 0.9). There are small differences in the region of lower overpotentials that could indicate a different kinetic route, although the uncertainty in measuring these small i_S values is much higher. The normalized curve was fit with the one simulated for these conditions by manually changing the values of k_o and α. The complete curve could not be correlated with the simple model adopted in this work. However, a good correlation was obtained using $k_o = 2.76 \times 10^{-9}$ cm/s and $\alpha = 0.65$ (or a Tafel slope $b = 0.09$ V/dec) over the region of potentials $0.7 < E_S$ (V) < 0.81 V, where the simple model would more properly describe this reaction. In terms of exchange current density ($j_o = nFk_oc_{O_2}$), assuming an O_2 solubility at 1 atm equal to 1.3 mM in phosphoric acid,[36] the calculated value is $j_o = 1.4 \times 10^{-9}$ A/cm^2. More evidence can be obtained by analyzing the experimental effects of the geometric conditions. Figures 10−12 show polarization curves obtained with different values of RG, L, and STR, respectively. A very interesting property results from the ability to change these geometric parameters. It is possible to obtain precise current measurements at lower overpotentials, where the reaction is slow, by performing experiments with the tip very close to the substrate.

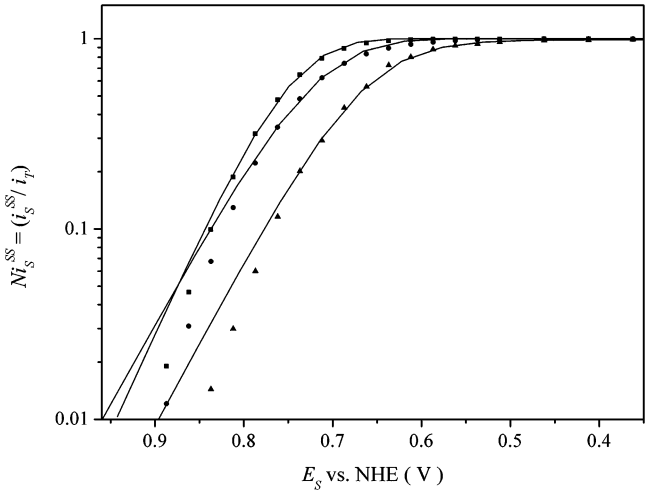

Figure 10. Dependence of the normalized steady-state substrate current on the substrate potential, obtained from ORR TG−SC experiments on a 127-μm Pt disk using 25-μm Pt tips with different RG values. $L \cong 0.8$, RG ≅ 2 (▲), 6 (●), and 10 (■). Solid lines: simulations (see Table 3).

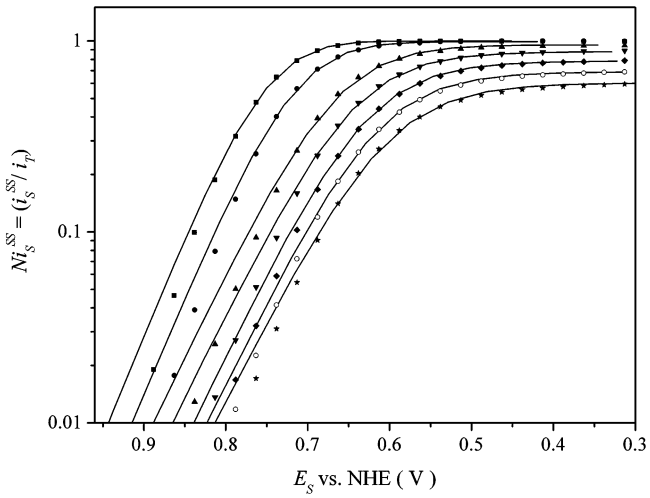

Figure 11. Dependence of the normalized steady-state substrate current on the substrate potential, obtained from ORR TG−SC experiments on a 127-μm Pt disk using a 25-μm Pt tip at different tip−substrate distances. RG ≅ 10, $L = 6.00$ (★), 5.08 (○), 4.16 (◆), 3.24 (▼), 2.32 (▲), 1.4 (●), and 0.94 (■). Solid lines: simulations (see Table 3).

On the other hand, it is possible to acquire information at more negative potentials, where normally the response is mixed or mass-transfer controlled, by decreasing the size of the substrate. The correlations with the simulated curves over restricted ranges of potentials ($\Delta E < 0.3$ V) are very good despite the very simple model used for the electrode reaction. Except with the results obtained using small substrates, the calculated values of j_o vary between 10^{-8} and 10^{-9} A/cm^2 (see Table 3). These values are larger than those reported in the literature for the same conditions,[33] though it is known that preactivated electrodes show higher nonstable activity.[38] The values of α (or b) spread in the range $0.5 \le \alpha \le 0.65$ ($0.09 \le b$ (V/decade) ≤ 0.118), in agreement with those obtained on polycrystalline[39] and single-crystal Pt

(38) Appleby, A. J.; Borucka, A. *J. Electrochem. Soc.* **1969**, *116*, 1212.
(39) Hsueh, K.-L.; Chin, D.-T.; Srinivasan, S. *J. Electroanal. Chem.* **1983**, *153*, 79.

Table 3. Kinetic Parameters of the ORR Resulting from Correlations between Simulated and Experimental Polarization Curves Obtained by the TG−SC Mode

	conditions			well-fitted potential range (V vs NHE)	calculated kinetic parameters	
data source	L	RG	STR		j_o (A/cm^2)	α (b(V/dec))
Figure 9	0.79	10	5	0.81−0.70	1.4×10^{-9}	0.65 (0.091)
Figure 10	0.8	10	5	0.81−0.65	1.8×10^{-9}	0.61 (0.097)
		6		0.75−0.60	1.65×10^{-8}	0.50 (0.118)
		2		0.73−0.53	1.25×10^{-8}	0.515 (0.115)
Figure 11	0.94	10	5	0.80−0.65	3.1×10^{-9}	0.63 (0.094)
	1.40			0.76−0.61	2.8×10^{-9}	0.608 (0.097)
	2.32			0.71−0.51	7.2×10^{-9}	0.53 (0.112)
	3.24			0.69−0.46	7.2×10^{-9}	0.52 (0.114)
	4.16			0.66−0.44	5.3×10^{-9}	0.525 (0.113)
	5.08			0.66−0.40	5.2×10^{-9}	0.52 (0.114)
	6.00			0.66−0.40	7.2×10^{-9}	0.50 (0.118)
Figure 12	0.8	10	5	0.80−0.65	2.6×10^{-9}	0.59 (0.100)
			2	0.79−0.51	4.5×10^{-9}	0.57 (0.104)
			1	0.75−0.35	9.03×10^{-8}	0.45 (0.131)
			0.4	0.70−0.30	6.62×10^{-7}	0.34 (0.174)

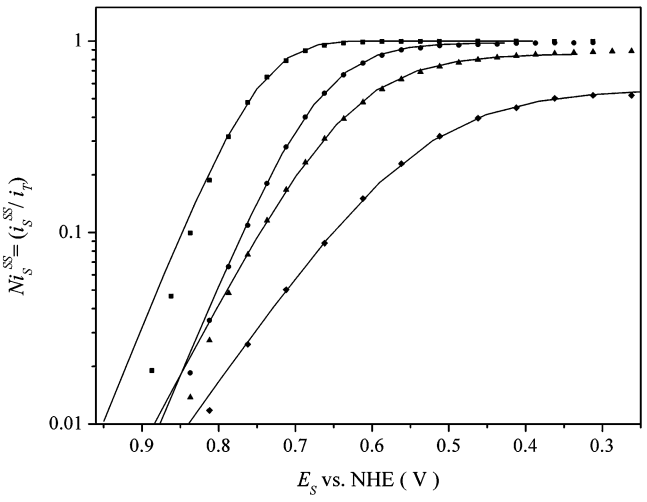

Figure 12. Dependence of the normalized steady-state substrate current on the substrate potential, obtained from ORR TG−SC experiments on Pt disks with different radii using a 25-μm Pt tip. RG ≅ 10, L ≅ 0.8, STR = 0.4 (◆), 1 (▲), 2 (●), and 5 (■). Solid lines: simulations (see Table 3).

electrodes[40] in about the same domains of potentials. However, the curve fitting obtained on the smaller substrates (STR = 1 and 0.4), although very good, leads to very high values of j_o and b. These facts reveal the necessity of a more complex model for the ORR that would be able to reproduce all the responses with a unique set of kinetic parameters.

CONCLUSIONS

The TG−SC mode of SECM is a valuable technique for performing kinetic studies of electrode reactions that are inaccessible to the feedback mode. A completely explicit highly versatile FD algorithm was designed to perform simulations of this SECM configuration, which can be easily adapted to simulate other SECM experiments. This mode of operation offers at least three approaches to carrying out kinetic studies. The analysis of the transient responses, while more complicated from an experimental point of view, would allow the study of fast reactions. A second possibility, the interpretation of steady-state polarization curves, was explored in detail in this work. A third approach is the analysis of TG−SC approach curves.

For a first-order, irreversible reaction, the TG−SC responses are independent of the tip current. The ability to easily change the geometric parameters of the experiment (L, STR, RG of the tip) provides a way to obtain a large number of independent experimental results that extend over a wide range of potentials. This property is a powerful tool in testing the self-consistency of a proposed mechanism.

The steady-state responses were used for the experimental determination of the heterogeneous rate constant for the ORR on preactivated, smooth Pt in phosphoric acid solutions. The reaction was assumed to operate by a simple first-order, irreversible reaction pathway. Correlations between steady-state simulated curves and experimental ones were good over certain ranges of potentials. The self-consistency of the model was checked by analyzing the spread of the kinetic parameters obtained under different geometric conditions. A more elaborate reaction mechanism, however, is required for the model to improve its descriptive capability over a wider range of conditions.

ACKNOWLEDGMENT

This work has been supported by grants from the National Science Foundation (CHE 0109587) and the Robert A. Welch Foundation. J.L.F. is grateful to the Fundación Antorchas (Argentina) for a postdoctoral fellowship.

SUPPORTING INFORMATION AVAILABLE

Simulation results obtained for varied geometric parameters (RG, L, STR). This material is available free of charge via the Internet at http://pubs.acs.org.

Received for review December 19, 2003. Accepted February 18, 2004.

AC035518A

(40) Kita, H.; Lei, H.-W.; Gao, Y. *J. Electroanal. Chem.* **1994**, *379*, 407.